jet INTL JOURNAL OF ELECTRONICS AND TELECOMMUNICATIONS, 2025, VOL. 71, NO. 4, PP. 1–7
Manuscript received September 9, 2025; revised October 2025. doi: 10.24425/ijet.2025.155455

Hardware implementation of MBFSK modulation technique for underwater wireless communications

Rafał Pilarski, and Łukasz Wojewódka

***Abstract*—The underwater communication technique based on MBFSK (Multiple Binary Frequency Shift Keying) modulation is used in challenging propagation conditions. Despite the bandwidth limitations present underwater, it provides stable underwater connectivity. This paper presents a hardware implementation of the MBFSK modulation technique for underwater wireless communications. The implementation was carried out using an FPGA-based programmable logic device. The concept of the device design, the hardware solution, and the firmware description are presented. An overview and diagram of the underwater communication system are also provided. The transceiver system was tested in the tank of the Hydroacoustics Laboratory of the Gdynia Maritime University, and the results are presented and discussed. The aim of this work is to present the design, software algorithm, and test results of the developed underwater communication system.**

***Keywords*—underwater communication; underwater acoustic communication; multipath channels; MBFSK, hardware implementation; FPGA**

I. Introduction

THE oceans cover about 71% of Earth's surface. The majority of life on Earth is found in the oceans, making them a key component of our planet's ecosystem [1]. The aquatic environment is inherently unfriendly to both human and machine. The main reason for this is the high pressure, which increases with depth and poses a serious challenge to people, equipment, and technology, which must be extremely robust to survive in such conditions. Another condition is the temperature, which is relatively low, especially in deeper waters, and can cause equipment failure if not properly adapted to such conditions. Moreover, seawater is highly corrosive, especially in areas with high salinity, which accelerates the corrosion of machinery, vessels, and equipment. Limited natural light in the deep ocean further complicates visual analysis and optical sensing. Additionally, ocean currents and waves can impact the stability of ships and submerged systems, while strong winds and storms often disrupt human activities in open sea regions.

Although the oceans cover a large part of the Earth's surface, they remain a challenge to study thoroughly. Despite extensive research efforts, only about 20 percent of the oceans have been comprehensively explored, leaving the rest largely unknown. Even with technological advances, many of the mysteries of these waters remain undiscovered. Ocean exploration is vital not only for scientific reasons (e.g. climate change research, marine ecosystems), but also for economic (search of natural resources) and military strategic reasons. The challenges of depth, pressure, temperature, and accessibility mean that a complete understanding of the oceans requires advanced technology and a long-term commitment.

Underwater communications systems can be implemented using various transmission techniques. A survey [2] lists several modulation techniques used in the UWA (underwater acoustic) channel. Most approaches employ OFDM (orthogonal frequency-division multiplexing) technique or its derivatives. In [3], the authors propose an adaptive algorithm for OFDM signals transmitted in time-varying, Doppler-distorted multipath channels. The proposed algorithm enables low-complexity post-FFT phase tracking and adaptive MMSE (minimum mean square error) combining of signals received across an array. The authors of [4] implemented TDS-OFDM (time-domain synchronization OFDM) transmission technique with a compressive sensing channel estimation algorithm and conducted a sea measurement trail over the distance of 1 kilometer. The paper [5] proposes a C-BCH (ciphered Bose-Chaudhuri-Hocquenghem) encoded OFDM scheme that uses predetermined keys to minimize the PAPR (peak-to-average power ratio) in an N-subcarrier system. This approach allowed a significant PAPR reduction of up to 12 dB. In [6], [7] an OFDM transmission technique was implemented in hardware. The former paper [6] describes the design and implementation of an MFSK-OFDM (Multiple Frequency Shift Keying OFDM) modem using FPGA architecture. By utilizing parallel computing, the authors developed a real-time communication system. With the use of Turbo codes, the proposed system achieved error-free transmission. The second paper [7] adopted the same modulation technique but implemented it on an ARM architecture. The use of this processor resulted in an energy-efficient solution. Coherent transmission techniques produce significantly higher data rates than their non-coherent counterparts; however, they require precise channel synchronization and equalization [2]. In heavy multipath environment, as shown in [8], coherent techniques can perform worse in terms of BER (bit error rate). The authors of [8]–[10] propose non-coherent modulation techniques, such as MBFSK (Multiple

This work was supported by the National Centre for Research and Development under Project DOB-SZAFIR/01/B/017/04/2021.

R. Pilarski is with Doctoral School, Gdynia Maritime University, Gdynia, Poland (e-mail: r.pilarski@sd.umg.edu.pl).

Ł. Wojewódka is with Faculty of Electrical Engineering, Gdynia Maritime University, Gdynia, Poland (e-mail: l.wojewodka@we.umg.edu.pl.

Binary Frequency Shift Keying). In the presence of movement and multipath effects over short distances, these method can achieve near error-free transmission.

One of the essential elements of the ability to work underwater in any application, i. e. marine research, rescue and maritime operations, search and exploration, situation monitoring, including ensuring the safety of critical infrastructure, underwater tourism, is the provision of communication with objects in the water. Traditional methods of communication, such as wired connections, are difficult to use in aquatic environment due to the high resistance of cables moving in water, problems with cable unwinding and the effect of water on cable materials. Therefore, enabling underwater wireless communications is important for a number of reasons, mainly related to safety, efficiency and the requirements of modern marine technology. Acoustic waves are commonly used for underwater wireless communications because they can propagate over relatively long distances, while radio frequency waves are heavily absorbed in the water environment [11]. This technique is relatively easy to implement but has its limitations, particularly in terms of throughput. Research is therefore still underway to improve underwater communication technology. This paper is in line with the current research trend to develop and study solutions to improve the quality, in terms of low error rate and high throughput, of underwater data transmission. The objective of the work carried out was the design of the hardware layer and the implementation of the MBFSK modulation technique, selected as suitable for providing communication in harsh propagation conditions. As a result of the research, an FPGA-based solution was developed to provide point-to-point, short range communication in a hydroacoustic channel under difficult propagation conditions. Additionally, this work aimed to achieve the maximum transmission speed while maintaining an acceptable error rate, as determined by the adopted BCH coding. The developed solution was tested in laboratory conditions and the results obtained confirmed the correctness of the adopted and applied solutions, in particular they enabled stable underwater communication with low error rates and acceptable throughput.

The article is divided into 6 chapters describing the various topics covered in the paper. Chapter two discusses the MBFSK modulation technique in detail. Chapter three describes the hardware implementation of the MBFSK modulation technique. Chapter four presents the firmware algorithm of the FPGA chip. Chapter five presents an underwater communication system based on the developed hardware solution. Chapter six describes how the laboratory trials were carried out, presents the results obtained, and draws conclusions based on these results. It concludes with a brief summary of the work carried out and also indicated further research directions.

II. Transmitted signal

The MBFSK modulation technique is an extension of the classic BFSK (Binary Frequency Shift Keying) modulation, where the number of bits transmitted per symbol is multiplied. Each data bit corresponds to two subcarriers, with the value of the bit determined by which subcarrier is active. The

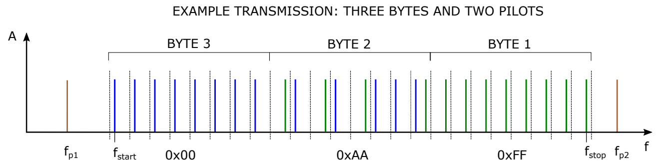

Fig. 1. An example of the spectrum form of the MBFSK modulation technique

subcarriers transmitted simultaneously form a symbol. The receiver determines the value of the bit based on a comparison of the spectral density at the frequencies corresponding to the bit. If the value of the amplitude spectrum is higher at the position with a higher frequency, it means the value ”1”, while at a lower frequency it means the value ”0”. In the transmitter, the phases of the individual subcarriers are randomized in order to minimize the PAPR parameter. The individual bits are transmitted according to an assumed frequency grid that should ensure orthogonality of the subcarriers [12]. An important parameter when defining this spacing is the distance in the frequency domain between the individual subcarriers f_{dn}. This parameter, together with the bandwidth occupied by the symbol B, determines the number of bits L_{bit} that can be transmitted in a single symbol so that the relation (1) is satisfied:

$$B = 2f_{dn}L_{bit}. \tag{1}$$

This, in turn, translates into throughput. The smaller the f_{dn}, the higher the throughput. However, the f_{dn} parameter must be chosen carefully, as too small a value will cause interbit interference, mainly due to Doppler spread.

Pilots are also placed at specific frequencies within the symbol. They are used to estimate the Doppler shift. Their placement in the frequency domain depends on the assumed maximum mutual velocity of the communicating transmitter-received objects. The pilot frequencies must be chosen so that, despite the Doppler shift, they do not overlap with the frequency range intended for the transmitted data. An example of the MBFSK modulation spectrum is shown in Fig. 1. It includes two pilots (f_{p1} and f_{p2}) and an example of three bytes with values of 0x00, 0xAA, and 0xFF. The vertical dashed lines indicate the boundaries of each bit.

In the frequency domain, a synchronization signal in the form of a LFM (Linear Frequency Modulation) signal, known as a chirp, is generated with the pilots before each transmitted symbol. This enables the receiver to detect the transmission and estimate the propagation conditions of the acoustic wave. This can be used to select transmission parameters, such as the guard time between symbols t_g, to achieve the highest quality transmission. A chirp signal is detected when a predefined threshold is exceeded at the output of the matched filter to which the received signal is applied. The time, at which the output of the matched filter drops below a certain threshold corresponds to the channel memory time. This can be used to determine the appropriate guard time. The chirp signal with adjustable parameters (such as start and end frequency, time duration t_{ch} and time interval between the chirp signal

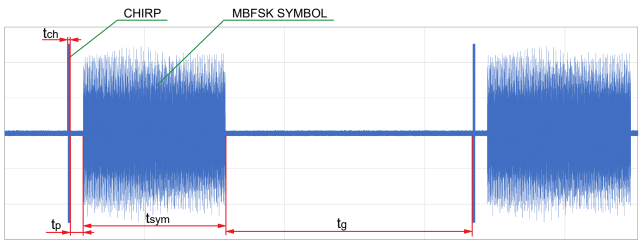

Fig. 2. An example of the signal time waveform

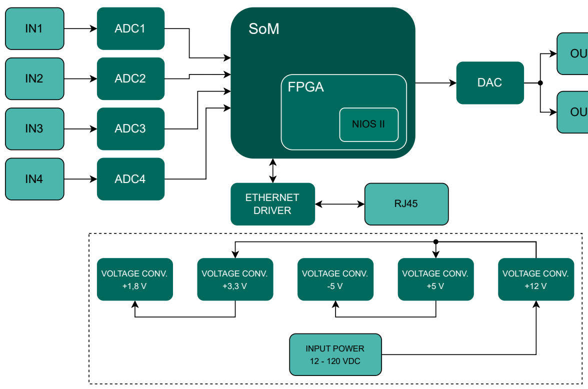

Fig. 3. Block diagram of the Hydroacoustic Transmission Module

and the transmitted data t_p) is transmitted in the band not occupied by the symbol. The MBFSK symbol is followed by a transmission interval t_g, which is derived from the duration of the impulse response in a given propagation channel. This limits the phenomenon of ISI (Intersymbol Interference) [13]. An example of the signal described is depicted in Fig. 2.

III. Hardware Implementation of the MBFSK Modulation Technique

The hardware implementation of the MBFSK modulation technique was based on a FPGA (Field Programmable Gate Array) architecture. The transmission device was designed as a transmitter-receiver circuit, hereafter referred to as the MTH module (Hydroacoustic Transmission Module). The module was fabricated as a 6-layer PCB (Printed Circuit Board) to which a SoM (System on Module) with an Intel Cyclone 10 GX FPGA control chip was connected via board-to-board connectors. The device was equipped with four 16-bit AD4001 ADCs (Analogue-to-Digital Converter), a 16-bit DAC8811 DAC (Digital-to-Analogue Converter), an on-chip programmer and an Ethernet controller based on the Wiznet W5200 chip. Five power sources are located on the base board: +12 V, +5 V, -5 V, +3.3V, and +1.8 V. The block diagram of the device is presented in Fig. 3.

The module was designed in the Altium Designer, while the FPGA chip was configured and programmed in the Quartus Prime Pro. The device was attached to an aluminium structure, which allowed it to be mounted in a sealed tube designed for immersion in water. A view of the MTH module is shown if Fig. 4.

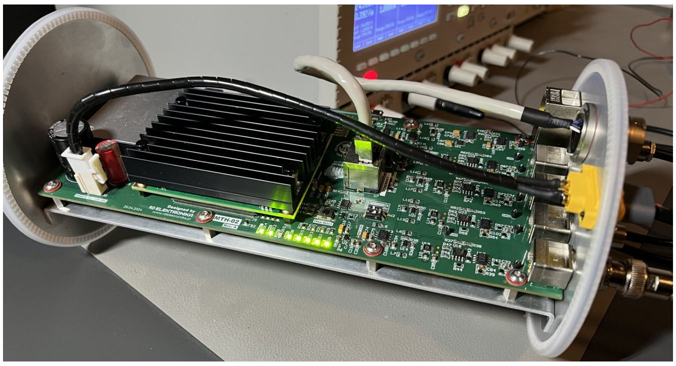

Fig. 4. Picture of the Hydroacoustic Transmission Module

The MTH module is configured and controlled using a dedicated application developed in the Python programming environment and installed on a host computer connected to the module via LAN. Communication between the module and the application is based on the UDP (User Datagram Protocol). The Nios II embedded processor, implemented within the FPGA structure, is responsible for handling the transmission protocol between the MTH module and the computer. The developed communication protocol enables the module to interface with various programming environments, such as MATLAB. A dedicated communication protocol has been developed for this communication, which provides a software interface for the module. Besides transmitting and receiving data, the external application also allows configuration of nearly all parameters related to the MBFSK modulation and the chirp signal.

The FPGA module on the transmitting side generates samples of the MBFSK signal during the modulation process. Demodulation process is performed using the FFT (Fast Fourier Transform). The module has the ability to acquire signals from four channels, each from a separate receiving hydrophone. Receiving begins once the chirp signal is detected. The MTH is a universal module and allows the implementation of other modulation techniques.

IV. Firmware Description

A simplified functional diagram of the signal forming circuit in the transmission path is shown in Fig. 5. The circuit's task is to convert the input binary information into a modulated MBFSK signal.

The diagram shows the input conversion algorithm. The first stage of the software operation is the generation of pseudo-random numbers by the Nios II embedded processor. These numbers represent random initial phases for the generated sinusoidal signals and are stored in the PHASE MEM memory cells. The Nios II processor determines a frequency grid for the binary values "0" and "1" based on the start and end frequency values and the number of bytes to be transmitted. These values are stored in the INC MEM memory cells and represent the sampling period of each subcarrier for subsequent time samples.

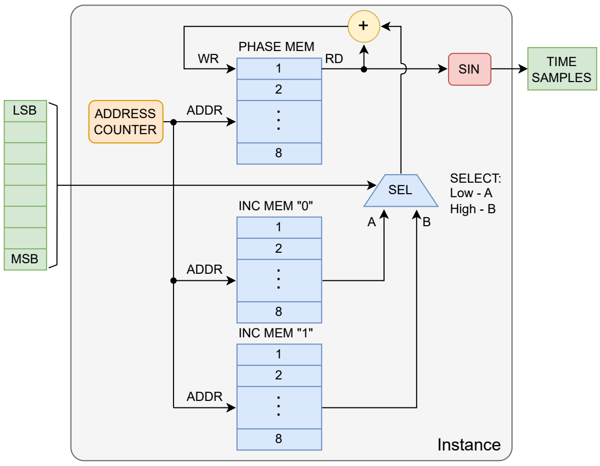

Fig. 5. A simplified functional diagram of the FPGA firmware on the transmitter side

The above steps are repeated each time the transmitter parameters are changed.

In the first stage of the conversion algorithm, a value is read from the first cell of PHASE MEM memory, representing the random initial phase of the first subcarrier frequency. This value is then incremented by the first value from the INC MEM memory. If the bit is 0, the value is read from the INC MEM ”0” memory, while if it is 1, the value is read from INC MEM ”1” memory. The result of the summation of the random initial phase and the sampling period overwrites the previous value in the PHASE MEM memory. The updated value is then applied to the input of the sin function, producing the first value of the first subcarrier, according to the frequency grid shown in Fig. 1. Similarly, subsequent bits of the transmitted data string are processed, resulting in the first time samples of the subsequent subcarriers. All time samples calculated in this manner are summed up to form the first time sample of the MBFSK signal.

For each subsequent time sample, the algorithm works in the same way, except that the initial phase values are no longer used. Instead, the instantaneous phase of the previous time sample stored in PHASE MEM memory is utilized. The sampling period value from the corresponding INC MEM memory cell is then added to this value.

The operation of the conversion circuit is synchronized by the ADDRESS COUNTER, which sequentially switched the individual memory cells and retrieves the next data bits. The clock frequency of the modulator circuit is 180 MHz.

For optimization purposes, the conversion of individual data bytes is performed in parallel by independent instances. The entire process of calculating single sample of the MBFSK signal, regardless of the number of data bytes, is much shorter than the sampling time of the DAC. At a sampling frequency of 1.2 MHz, this duration is less than 1 µs.

The receiver circuit, which performs the FFT function, uses the IP-Core megafunction implemented in the FPGA. A simplified functional diagram of the FPGA firmware on the receiver side is shown in Fig. 6

The hydroacoustic signal received by a set of four hydrophones is fed, after amplification and pre-filtering, to the inputs of four independent ADCs operating at 400 kHz. The signal from each hydrophone is directed to the input of a dedicated CHIRP DETECTOR module which includes a MATCHED FILTER and a PEAK VALUE DETECTOR. The purpose of this filter is to accurately determine the start of a useful signal. It is a linear filter whose impulse response is determined by conjugating time reversed input signal [14], i.e. the chirp signal, according to equation (2):

$$h(t) = s^*(T - t), \tag{2}$$

where $h(t)$ is the impulse response of a matched filter, T is the signal duration, and $s^*(t - T)$ is the conjugated time reversed input signal.

The signal from the filter output is then passed to the peak detector, which uniquely identifies the received signal as the beginning of the transmission. The signals from all four channels are fed to an OR gate, where the first correctly identified signal from any of the four CHIRP DETECTOR modules initiates further processing.

The module that controls the data processing is the STATE MACHINE, which initially waits for the synchronization signal indicating the start that determines the beginning of the received signal. After detecting the beginning of the signal, the STATE MACHINE writes 16-bit samples from all channels into the SAMPLE MEMORY. The number of samples required for a Fourier transform by the IP-Core megafunction used is 2^{14}, i. e., 16384.

After storing all the samples, the STATE MACHINE retrieves the samples for each channel from the memory and feeds them into the input of the FFT IP-Core megafunction. The result of the transformation is complex numbers, from which the modulus, i.e., the amplitudes of the individual frequencies of the transmitted signal, are determined. The STATE MACHINE writes the data to the DUAL-PORT MEMORY, which acts as an interface between the FPGA chip and the Nios II embedded processor. The processor then transmits the received and processed data via Ethernet to an external application.

To keep up with the data stream, all data processing is performed at a clock rate of 100 MHz. This organization of the FPGA software structure enables the FFT transformation for all four channels to be completed within a single milliseconds.

V. Underwater communication transceiver

Based on the hardware implementation of MBFSK modulation, an underwater communication transceiver has been developed. Its block diagram is shown in Fig. 7. The set of two transceivers provides a point-to-point wireless underwater communication link. The receive path uses four Neptune B/200 hydrophones connected to an FPGA module via an Etec A1105 amplifier. The transmit path uses one Neptune B/200 and one Neptune T226 hydrophones connected via a Benthowave BII5021 power amplifier to the output of the

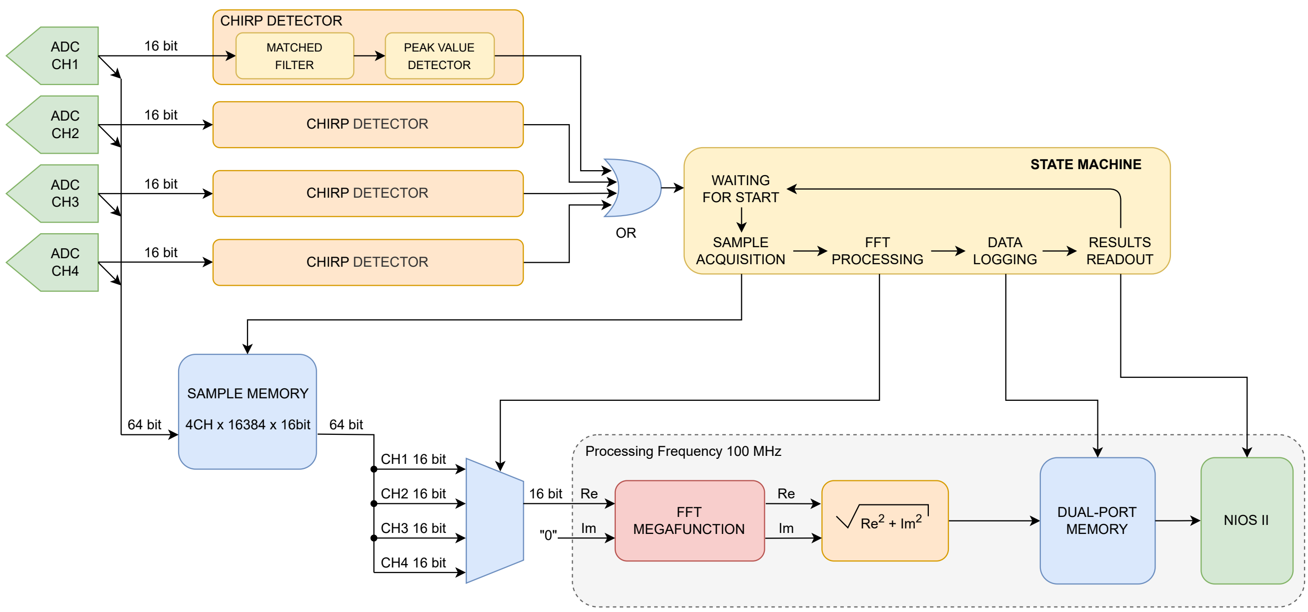

Fig. 6. A simplified functional diagram of the FPGA firmware on the receiver side

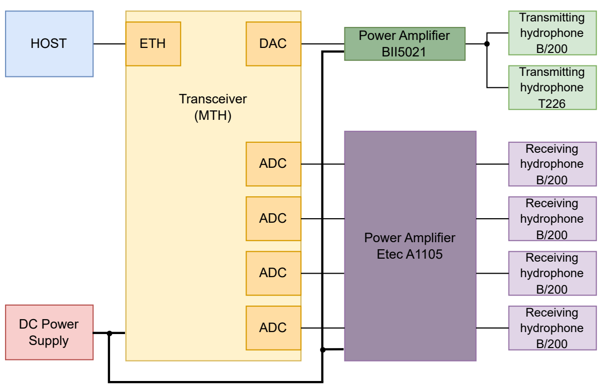

Fig. 7. Block diagram of the underwater communication transceiver

FPGA module. The use of four hydrophones on the receiver side helps mitigate fading through collective reception. This is achieved by summing the amplitude spectra obtained from the four hydrophones [15]. Since MBFSK is a non-coherent transmission scheme, it does not require precise phase synchronization between hydrophones. The use of two hydrophones on the transmitter side allows the desired transmission characteristics to be achieved within the frequency band used for data transmission. One hydrophone has a transmitting characteristic centered around 60 kHz, while the other is centered around 110 kHz.

A dedicated transmission protocol has been developed for communication between the MTH module and the host computer. This protocol involves the exchange of well-defined messages. The header preceding each message is responsible for identifying the type of message. This allows the transmitter and receiver parameters to be defined and the amplitude spectra of the received signals to be received. The host computer performs the collective reception and transforms the amplitude spectra acquired by the MTH module into a sequence of bits.

The developed protocol allows for the definition of following parameters related to the MBFSK modulation and the chirp signal:

- start and end frequency of the chirp signal,
- duration of the chirp signal t_{ch},
- time interval between the chirp signal and the transmitted data t_p,
- frequency of each pilot f_{pn},
- start and end frequency of the MBFSK modulation,
- number of bytes N transmitted in a symbol, ranging from 1 to 64,
- duration of the MBFSK symbol t_{sym},
- time interval between successive symbols transmitted, guard time t_g,

Additionally, on the receiver side, it is possible to detect the time after which the signal level drops at the output of the matched filter. This makes it possible to determine the channel memory time, which is useful for determining the appropriate guard time.

VI. Testing in Laboratory Conditions

The validation of the adopted solutions was verified during tests in the tank of the Hydroacoustics Laboratory at Gdynia Maritime University. Two sets of hydrophones were placed in a tank with a capacity of 11.5 m^3 and dimensions of 3.78 x 1.75 x 1.6 m, positioned 1.3 m apart, as presented in Fig. 8.

The research was carried out under stationary conditions. The tank has difficult propagation conditions due to a strong multipath effect. An estimate of the absolute value of impulse response of the hydroacoustic channel is shown in Fig. 9.

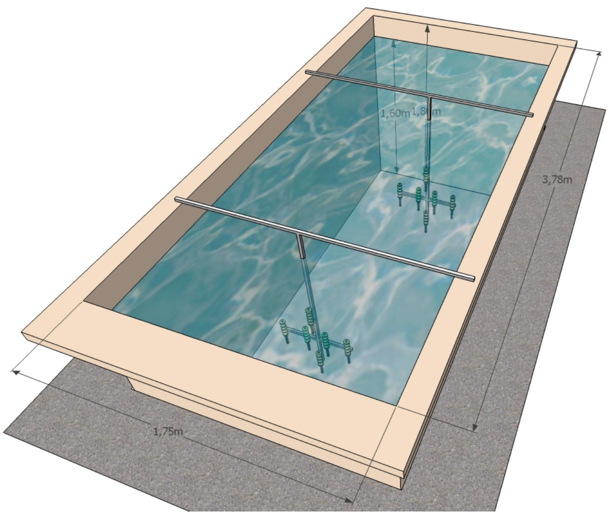

Fig. 8. A tank with placed hydrophones

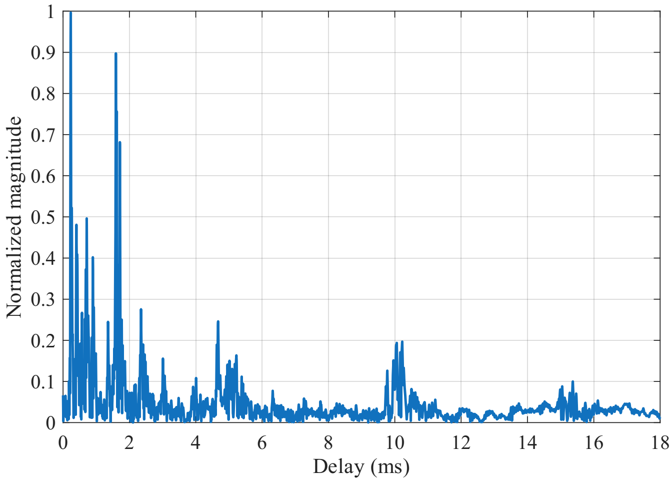

Fig. 9. Estimate of the absolute value of impulse response of the hydroacoustic channel in the Gdynia Maritime University laboratory tank

During tests, the transmission quality, expressed in terms of BER (bit error rate) and PER (packet error rate) was studied as a function of the transmission parameters, i.e. the frequency spacing f_{dn}, the number of hydrophones used for collective reception NoH and applied guard time t_g. The transmission used BCH correction coding with parameters n = 511, and k = 421, allowing for the correction of up to 10 errors for an MBFSK symbol length of $N_{bs} = 480$ bits. However, it was not possible to transmit all 511 bits within a single frame. Since the encoded sequence includes the original information bits, zero-padded was applied to the encoded data. A known number of zeros, which were not transmitted, were later restored by the receiver to enable proper decoding. An analogous procedure was applied for other values of the N_{bs} parameter. If BCH decoding failed to correct the received frame, the frame was discarded and counted toward the PER. Otherwise, the frame was accepted,

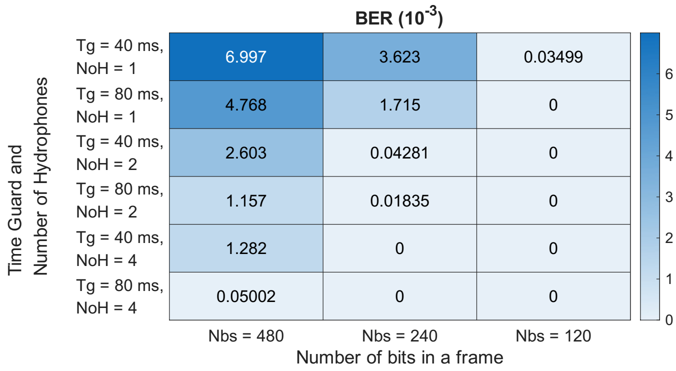

Fig. 10. BER heatmap showing the effect of different time guards, the number of hydrophones, and the number of bits in a frame.

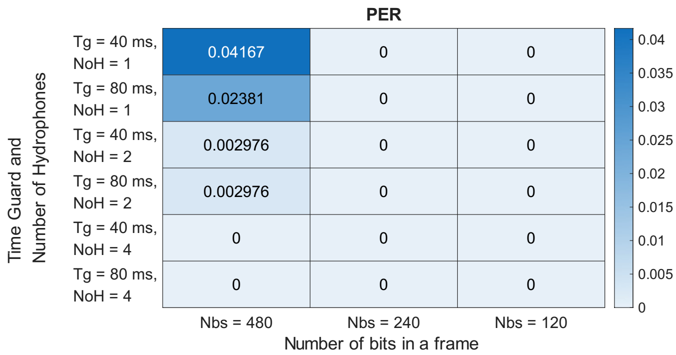

Fig. 11. PER heatmap showing the effect of different time guards, the number of hydrophones, and the number of bits in a frame.

and the number of corrected bits was included in the BER calculation.

Three measurements were performed for each transmission parameter setting, each consisting of the transmission of 10,000 bytes. The transmission was conducted in the frequency range from 53.125 kHz to 146.875 kHz and the duration of the MBFSK symbol t_{sym} was 40.96 ms. The transmission parameters, are shown in the Table I. Transmission rates were measured using configurations with four receiving hydrophones and calculated based on the number of bits per MBFSK symbol N_{bs}, excluding bits reserved for BCH coding. The summarized results are presented as a heatmaps in Fig. 10 and Fig. 11, representing the arithmetic mean of all the tests carried out for each parameter set.

TABLE I
TRANSMISSION PARAMETERS

t_g (ms)	f_{dn} (Hz)	Nbs	Transmission rate (kb/s)
40	97.66	480	4.06
40	195.31	240	2.17
40	390.63	120	1.03
80	97.66	480	2.85
80	195.31	240	1.51
80	390.63	120	0.72

The number of hydrophones used for collective reception is important for the BER. Increasing the number of receiving hydrophones has a positive impact on reception quality, reducing both the BER and PER. The use of four receiving hydrophones resulted in the successful reception of all transmitted frames.

Preliminary studies of the MBFSK modulation technique [8] indicate that the subcarrier spacing has a significant impact on transmission quality. From the figures shown, it can be seen that decreasing the frequency spacing results in an increase in both BER and PER. According to Fig. 11, the BCH coding corrects all errors when the number of bits per symbol Nbs reaches 240. However, it should be noted that this parameter affects the transmission rate. During the tests, with four hydrophones, a result of 4 kb/s was obtained.

The impact of the guard time T_g on the transmission quality can be observed. The resulting BER decreases when T_g is doubled, due to reduced ISI

VII. Conclusions

The provision of wireless underwater communication is essential for effective underwater operations. For this reason, the MBFSK modulation technique was implemented in hardware to develop a transceiver capable of operating in challenging propagation conditions, such as those with strong multipath effects. The implementation was carried out using an FPGA-based programmable logic device. The developed transceiver was tested under laboratory conditions. Additional features, including collective reception and error correction coding, enable data transmission at rates of up to 4.06 kb/s. The hardware solution is versatile, it can be reprogrammed to support other modulation techniques and data transmission methods as needed.

Further testing of the transceiver will be conducted under strong multipath conditions, including scenarios involving relative motion between the transmitter and receiver. Field tests in freshwater environments are also planned. Additionally, optimization efforts are underway to increase the transceiver's data throughput.

References

[1] R. Stewart, *Introduction to Physical Oceanography*. University Press of Florida, 2009.

[2] N. U. R. Junejo, M. Sattar, S. Adnan, H. Sun, A. B. M. Adam, A. Hassan, and H. Esmaiel, "A Survey on Physical Layer Techniques and Challenges in Underwater Communication Systems," *Journal of Marine Science and Engineering*, vol. 11, no. 4, 2023. [Online]. Available: https://www.mdpi.com/2077-1312/11/4/885

[3] M. Stojanovic, "Low Complexity OFDM Detector for Underwater Acoustic Channels," in *OCEANS 2006*, 2006, pp. 1–6.

[4] N. U. R. Junejo, H. Esmaiel, M. Sattar, H. Sun, M. A. Khalil, and I. Ullah, "Sea Experimental for Compressive Sensing-Based Sparse Channel Estimation of Underwater Acoustic TDS-OFDM System," *Wireless Communications and Mobile Computing*, vol. 2022, no. 1, p. 2523196, 2022. [Online]. Available: https://onlinelibrary.wiley.com/doi/abs/10.1155/2022/2523196

[5] M. Murad, I. A. Tasadduq, and P. Otero, "Ciphered BCH Codes for PAPR Reduction in the OFDM in Underwater Acoustic Channels," *Journal of Marine Science and Engineering*, vol. 10, no. 1, 2022. [Online]. Available: https://www.mdpi.com/2077-1312/10/1/91

[6] Z. Tang, S. Tu, W. Huang, and Y. Zhang, "Design and implementation study of FPGA-based underwater acoustic MFSK-OFDM communication algorithm," in *International Conference on Image, Signal Processing, and Pattern Recognition (ISPP 2024)*, R. B. Pachori and L. Chen, Eds., vol. 13180, International Society for Optics and Photonics. SPIE, 2024, p. 131803S. [Online]. Available: https://doi.org/10.1117/12.3033604

[7] C. T. Tan GAO, Chengcai LYU, "Error control method for OFDM-MFSK underwater acoustic communication," *Systems Engineering and Electronics*, vol. 44, no. 5, p. 1701, 2022. [Online]. Available: https://www.sys-ele.com/EN/abstract/article_8667.shtml

[8] A. Czapiewska, A. Luksza, R. Studański, L. Wojewódka, and A. Zak, "Evaluation of Selected Modulation Techniques in Underwater Multipath Channel," *IEEE Access*, vol. PP, pp. 1–1, 01 2025.

[9] J. H. Schmidt, A. M. Schmidt, I. Kochańska, R. Studański, and A. Żak, "Performance of underwater data transmission using incoherent modulation MFSK in very shallow waters," *Int. J. Electron. Commun. Telecommun.*, vol. 70, pp. 861–869, 2024.

[10] A. Czapiewska, A. Łuksza, R. Studański, L. Wojewódka, and A. Żak, "Comparison of Doppler Effect Estimation Methods for MFSK Transmission in Multipath Hydroacoustic Channel," *IEEE Access*, vol. 12, pp. 49 976–49 986, 2024.

[11] U. M. Qureshi, F. K. Shaikh, Z. Aziz, S. M. Z. S. Shah, A. A. Sheikh, E. Felemban, and S. B. Qaisar, "RF Path and Absorption Loss Estimation for Underwater Wireless Sensor Networks in Different Water Environments," *Sensors*, vol. 16, no. 6, 2016. [Online]. Available: https://www.mdpi.com/1424-8220/16/6/890

[12] A. Czapiewska, A. Łuksza, R. Studański, L. Wojewódka, and A. Żak, "Evaluating the Effectiveness of Doppler Frequency Shift Determination using Pilots in Broadband Transmission," *Int. J. Electron. Commun. Telecommun.*, vol. 70, pp. 797–803, 2024.

[13] M. Hasan, M. Hossain, M. Islam, and R. Mondol, "Comparative study of different guard time intervals to improve the ber performance of wimax systems to minimize the effects of isi and ici under adaptive modulation techniques over sui-1 and awgn communication channels," *International Journal of Computer Science and Information Security*, vol. 6, 11 2009.

[14] H. Van Trees, K. Bell, and Z. Tian, *Detection Estimation and Modulation Theory, Part I: Detection, Estimation, and Filtering Theory*, ser. Detection Estimation and Modulation Theory. Wiley, 2013.

[15] J. Mizeraczyk, R. Studanski, A. Zak, and A. Czapiewska, "A Method for Underwater Wireless Data Transmission in a Hydroacoustic Channel under NLOS Conditions," *Sensors*, vol. 21, no. 23, 2021. [Online]. Available: https://www.mdpi.com/1424-8220/21/23/7825